International Journal of Nanomedicine

Dovepress
open access to scientific and medical research

Open Access Full Text Article

ORIGINAL RESEARCH

Graphene/single-walled carbon nanotube hybrids promoting osteogenic differentiation of mesenchymal stem cells by activating p38 signaling pathway

This article was published in the following Dove Press journal:
International Journal of Nanomedicine
20 October 2016
Number of times this article has been viewed

Xinxin Yan[1,2]
Wen Yang[3]
Zengwu Shao[1]
Shuhua Yang[1]
Xianzhe Liu[1]

[1]Department of Orthopaedic Surgery, Union Hospital, Tongji Medical College, Huazhong University of Science and Technology, [2]Department of Orthopaedic Surgery, Wuhan Third Hospital, [3]Department of Anesthesiology, Union Hospital, Tongji Medical College, Huazhong University of Science and Technology, Wuhan, People's Republic of China

Abstract: Carbon nanomaterials are becoming increasingly significant in biomedical fields since they exhibit exceptional physicochemical and biocompatible properties. Today, the stem cells offer potentially new therapeutic approaches in tissue engineering and regenerative medicine. However, the induction of differentiation into specific lineages remains challenging, which provoked us to explore the biomedical applications of carbon nanomaterials in stem cells. In this study, we investigated the interactions between graphene/single-walled carbon nanotube (G/SWCNT) hybrids and rat mesenchymal stem cells (rMSCs) and focused on the proliferation and differentiation of rMSCs treated with G/SWCNT hybrids. Cell viability and morphology were evaluated using cell counting kit-8 assay and immunofluorescence staining, respectively. Osteogenic differentiation evaluated by alkaline phosphatase activity of MSCs proved to be higher after treatment with G/SWCNT hybrids, and the mineralized matrix nodule formation was also enhanced. In addition, the expression levels of osteogenic-associated genes were upregulated, while the adipocyte-specific markers were downregulated. Consistent with these results, we illustrated that the effect of G/SWCNT hybrids on the process of osteogenic differentiation of rMSCs can be modulated by activating the p38 signaling pathway and inhibiting the extracellular signal-regulated kinase 1/2 pathway. Nevertheless, our study suggests that carbon nanomaterials offer a promising platform for regenerative medicine in the near future.

Keywords: carbon-based nanomaterials, 3D nanostructure, stem cell therapy, bone formation

Introduction

Current clinical challenges require new regenerative medicines for diseased and injured organs and tissue. The aim of regenerative medicine research is to develop potential therapeutics to restore or maintain their regular and normal function.[1,2] In orthopedic surgery, when osteonecrosis and nonunion bone fractures occur, there is little intrinsic repair ability, owing to poor regeneration potential. Stem cell therapy is considered a promising and effective approach in complex tissue regenerative studies. This therapy induces the stem cells into the desired cell lineage, but requires adequate extracellular microenvironment to regulate cell proliferation and differentiation.

Mesenchymal stem cells (MSCs) are bone marrow-derived cells that can differentiate into various mesodermal lineages, including osteoblasts, adipocytes, chondrocytes, and neurons, both in vitro and in vivo.[3] By self-renewal and multiple lineage differentiation capabilities, MSCs provides an ideal model system for applications in stem cell therapy and regenerative medicine. Moreover, MSCs are less likely to be rejected by

Correspondence: Xianzhe Liu
Department of Orthopaedic Surgery, Union Hospital, Tongji Medical College, Huazhong University of Science and Technology, 1277 Jiefang Road, Wuhan 430022, People's Republic of China
Tel +86 27 8535 1627
Fax +86 27 8535 1627
Email liuxianzhe@gmail.com

submit your manuscript | www.dovepress.com
Dovepress
http://dx.doi.org/10.2147/IJN.S115468

the host immune system and can be used as autologous grafts in stem cell therapy, especially for bone repair.[4–6] Therefore, it is critical to induce osteogenic differentiation of MSCs directed toward osteoblasts for using them in bone repair and regeneration. Because stem cell differentiation is controlled by the interaction between the extracellular microenvironment and the cells, the microenvironment around the stem cells, including the chemistry, micro-, and nanostructures, is important. Concerning this, there is still a large initiative to explore the nanostructure materials that promote osteogenic differentiation in stem cell therapy for new bone formation.

In an effort to enhance the differentiation of stem cells into lineage specification, nanostructure materials have elicited substantial attention in the fields of biological and regenerative medicine due to their physicochemical, biological, and biomimetic properties.[7,8] The combination of nanostructure materials and stem cell therapy offers a promising therapeutic option for promoting bone repair. Among the various kinds of nanomaterials, carbon nanomaterials have attracted great interest due to their applications in biomedical and biotechnological fields, including biological sensing,[9,10] gene and drug delivery,[11,12] cancer therapy,[13,14] and tissue engineering.[15,16] G/SWCNT hybrids, three-dimensional (3D) nanostructure carbon nanomaterials, have been in the forefront of numerous electrical and thermal conductive researches due to their extraordinary physicochemical properties. A 3D structure has been constructed by combining one-dimensional single-walled carbon nanotubes (SWCNTs) and two-dimensional (2D) graphene into 3D G/SWCNT hybrids. Graphene and SWCNTs can be expected to exhibit high surface area in the G/SWCNT hybrids.[17,18] Likewise, there is limited literature concerning the potential interference with the proliferation and differentiation processes of stem cells.

Recent studies on carbon nanomaterials have made great progress in demonstrating the differentiation ability of MSCs. It has been reported that graphene-based nanomaterials can promote the specific differentiation of MSCs into osteoblasts without hampering proliferation.[19] Graphene nanogrids can also serve as 2D selective templates to accelerate the differentiation of MSCs into osteogenic lineage, based on their excellent capability for adsorption of chemical inducers and the physical stresses induced by surface topographic features.[20] Carbon nanotubes exhibit the ability to improve cell attachment and proliferation, and also to differentiate human adipose-derived MSCs to osteogenic cells, since these carbon nanotubes are concentrated more on bone-inducing proteins and modulate downstream stem cellular response.[7] In addition to carbon nanomaterials, other types of nanomaterials, such as gold, titanium, silicon, and hydroxyapatite, also exhibit the potential to enhance differentiation.[8,21–23] The earlier studies contain crucial literature as a basis for further exploration of the possible uses of G/SWCNT hybrids for bone repair and regeneration using stem cells.

The mechanism of interaction between nanomaterials and MSCs has been previously investigated at a molecular level.[8,24] The p38 signaling pathway, a main family member of the mitogen-activated protein kinases (MAPK) pathway, plays an important role in a wide variety of biological processes, including cell development, death, and cell differentiation.[25] Many studies demonstrated that p38 MAPK can promote osteogenic differentiation.[26,27] The MAPK signaling pathway also has been implicated in stem cell proliferation and differentiation induced by nanomaterials. Gold nanoparticles promoted the differentiation of MSCs toward osteoblast cells by activating the p38 MAPK signaling pathway.[8] Silica nanoparticles increased the proliferation of human adipose tissue-derived stem cells by increasing the phosphorylation of p38 and extracellular signal-regulated protein kinase (ERK)1/2.[24]

In this paper, we aim to systematically investigate the interactive effects of G/SWCNT hybrids on the osteogenic differentiation of rat mesenchymal stem cells (rMSCs). We used cell counting kit-8 (CCK-8) assay and immunofluorescence staining techniques to study proliferation, morphology, and the cytoskeleton structures of rMSCs treated with G/SWCNT hybrids. Additionally, the effect of G/SWCNT hybrids on the differentiation toward osteoblasts and adipocytes was evaluated. Alkaline phosphatase (ALP) activity and mineralized matrix nodule formation were measured as specific markers of osteogenic differentiation of rMSCs at early and late stages. More importantly, we expand upon the exploration of the alteration of intracellular molecules to explain the possible underlying mechanisms of G/SWCNT hybrids effects on the differentiation processes of rMSCs.

Materials and methods

Preparation of G/SWCNT hybrids

G/SWCNT hybrids and SWCNTs were obtained from Beifang Guoneng New Material Co. Ltd. (Beijing, People's Republic of China). Graphene was purchased from Morsh Science and Technology Co. Ltd. (Ningbo, People's Republic of China). SWCNTs were synthesized by chemical vapor deposition processing using FeCo nanoparticles as catalysts and CH_4 as the carbon source under temperatures below 900°C, as described in a previous study.[17] SWCNTs were purified by washing FeCo nanoparticles with 37% HCl, followed by spray drying. The fabrication of the G/SWCNT hybrids was similar to the preparation method for SWCNTs,

but involved using FeMgAl catalytic nanoparticles instead of FeCo catalysis.[17] The as-prepared hybrids were also purified by 37% HCl, followed by a spray drying process to eliminate water. From the material's dealer, the characteristics of the synthesized G/SWCNT hybrids were obtained, which were as follows: 1) surface area: 1,676 m^2/g; 2) mean pore diameter: approximately 3.5 nm; and 3) porosity: around 63%.

The G/SWCNT hybrids dispersion was sonicated for 30 minutes (frequency =40 kHz) to minimize the heterogeneous intracellular responses before treating the cells. The stock solution of G/SWCNT hybrids was prepared at a concentration of 1 mg/mL using sterilized double-distilled water (dd-H_2O). Transmission electron microscopy (Hitachi Ltd., Tokyo, Japan) was used to characterize the morphologies and structures. Raman spectrum was obtained on confocal Raman microspectroscopy (RM-1000; Renishaw, Wotton-under-Edge, UK) at an excitation wavelength of 514.5 nm.

Cell culture and osteogenesis induction

MSCs were isolated from 6-week-old Sprague Dawley mice (Huazhong University of Science and Technology, Wuhan, People's Republic of China) using well-established methods.[28] This study and all animal experiments were approved by the Institutional Animal Care and Use Committee of Huazhong University of Science and Technology and were in accordance with the National Institutes of Health animal use guidelines. In brief, both ends of the femurs and tibiae were cut off at the epiphysis, and the marrow was flushed out using supplemented Dulbecco's Modified Eagle's Medium (DMEM)/F12 (Hyclone, Logan, UT, USA). rMSCs were collected and cultured in DMEM/F12 with 10% fetal bovine serum (Thermo Fisher Scientific, Waltham, MA, USA) and 1% penicillin/streptomycin (Thermo Fisher Scientific) at 37°C in 5% CO_2 atmosphere. At confluence, the cells were detached by 0.25% trypsin-ethylenediaminetetraacetic acid (Thermo Fisher Scientific). Cells were used in the following experiments at passage 3–4 and were maintained on the plate with a precoating of 1% gelatine solution (Cyagen, Guangzhou, People's Republic of China). For osteogenic differentiation, Sprague Dawley rat MSC osteogenic differentiation medium (Cyagen) was used and changed every 3 days. Cells treated with sodium fluoride (NaF) at 1 μM and without G/SWCNT hybrids were used as the positive and negative controls, respectively.[29]

CCK-8 assay

Cell viability and proliferation were determined using a CCK-8 assay kit (Dojindo, Kumamoto, Japan). Cells were seeded in a 96-well plate and incubated with culture medium containing different concentrations of G/SWCNT hybrids, grapheme, and SWCNTs for 24 hours. Cells were also incubated with G/SWCNT hybrids at different concentrations for 1, 3, and 7 days. At a predetermined time point, the culture media were removed and washed with phosphate-buffered saline (PBS) twice. Then, each well was replaced with 90 μL cell culture medium and 10 μL CCK-8 and was maintained for another 2 hours in the dark at 37°C. The absorbance was recorded at 450 nm using a microplate reader (BioTek, Winooski, VT, USA).

Immunofluorescence staining

Cellular morphology was determined using immunofluorescence staining. After the cells were seeded, they were cultured with cytochalasin D (Aladdin, Shanghai, People's Republic of China) for 30 minutes and then incubated with and without G/SWCNT hybrids for 24 hours. Next, the cells were fixed with 4% formaldehyde, permeabilized with 0.5% Triton X-100 at room temperature, and blocked with 1% bovine serum albumin (Sigma-Aldrich Co., St Louis, MO, USA). Cells were then rinsed with PBS three times and incubated in PBS including tetramethylrhodamine (TRITC)-phalloidin (Yeasen, Shanghai, People's Republic of China) at a final concentration of 100 nM in the dark for 30 minutes, according to the manufacturer's instructions. The cells were then counterstained with 4′,6-diamidino-2-phenylindole Fluoromount-G™ (Yeasen) for 5 minutes at room temperature. Images were collected using a confocal fluorescent microscope (LSM 780; Carl Zeiss Meditec AG, Jena, Germany).

ALP activity assay

ALP activity assay was performed according to the manufacturer's instructions (Jiancheng, Nanjing, People's Republic of China). Following a wash with PBS, the cells were lysed with 1% Triton X-100 (Beyotime, Shanghai, People's Republic of China) on each well. The lysate was collected with the aid of a cell scraper and centrifuged at 12,000 rpm for 15 minutes at 4°C to remove cell debris. Total protein content in the lysate was measured using a bicinchoninic acid assay kit (Jiancheng). The absorbance of samples was recorded at a wavelength of 562 nm using a microplate reader. Cell lysate was prepared as mentioned earlier, which proceeded for 15 minutes at 37°C, and then a developer was added. The absorbance was measured at 520 nm with a microplate reader using *p*-nitrophenol phosphate as the standard. All results were normalized by the total intracellular protein content, and thus expressed as units/g protein. One unit of enzyme is defined as the amount of enzyme that converts 1 g of protein to 1 mg of *p*-nitrophenol phosphate in 15 minutes at 37°C.

Alizarin red staining assay

The formation of mineralized matrix nodules was determined by alizarin red staining (ARS; Cyagen). After the cells were seeded, the culture medium was changed to the osteogenic differentiation medium in the presence or absence of G/SWCNT hybrids. In brief, samples were fixed in 4% paraformaldehyde for 30 minutes, following which they were washed in distilled water three times. Next, the samples were incubated with ARS solution for 5 minutes at room temperature. The staining was washed twice with distilled water and visualized using fluorescence microscope (CKX41; Olympus Corporation, Tokyo, Japan). For semi-quantification of ARS content, the stain was extracted by adding 10% cetylpyridinium chloride (Sigma-Aldrich Co.) for 30 minutes with constant shaking, and the ARS concentrations were determined by detection of the absorbance at a wavelength of 570 nm.

Oil red O staining

For adipogenic differentiation assay, Sprague Dawley rat bone marrow MSC adipogenic differentiation medium (Cyagen) was used in the protocol. The formation of adipocytes was measured by the oil red O staining (Cyagen) of lipid droplets. Cells were plated in 6-well plates and cultured with adipogenic differentiation medium in the presence or absence of G/SWCNT hybrids. At a desired time point, the cells were washed with PBS twice and stained with oil red O solution for 15 minutes. In order to quantify, the staining was dissolved in isopropyl alcohol and the absorbance was recorded at 510 nm using a microplate reader.

Western blot analysis

After incubating the G/SWCNT hybrids for 14 days, the cells were washed with PBS and harvested using the lysis buffer. Total protein was separated by 12% sodium dodecyl sulfate polyacrylamide gel electrophoresis and transferred to polyvinylidene difluoride membranes (EMD Millipore, Billerica, MA, USA). After washing three times, the membranes were incubated with the corresponding primary antibodies in Tris-buffered saline, 0.1% Tween 20 containing 1% bovine serum albumin solution overnight at 4°C, followed by incubation with secondary antibodies (Proteintech, Rosemont, IL, USA) for 60 minutes. The expressions of runt-related transcription factor 2 (Runx2; Proteintech), osteocalcin (OCN; Abcam, Cambridge, MA, USA), osteopontin (OPN; Abcam), peroxisome proliferator-activated receptor-γ2 (PPARγ2; Abcam), p38 (Epitomics, Burlingame, CA, USA), p-p38 (CST, Danvers, MA, USA), c-Jun-NH_2-terminal kinases (JNK; CST), p-JNK (CST), ERK1/2 (Bioworld, Minneapolis, MN, USA), and p-ERK1/2 (Bioworld) were visualized using an enhanced chemiluminescence detection system (Beyotime).

Statistical analysis

Data were expressed as mean ± standard deviation (SD) of at least three independent experiments. Statistically significant values were defined as $P<0.05$ (95% confidence interval) based on a two-tailed Student's *t*-test.

Results

Characterization of G/SWCNT hybrids

From the transmission electron microscopy image of the G/SWCNT hybrids, the expected 3D nanostructure was confirmed (Figure 1A). Figure 1B shows the Raman spectrum curve of the G/SWCNT hybrids. The peak appearing at the location of 100–250 cm^{-1} corresponds to the radial breathing mode peak of SWCNTs. Two near peaks emerging at the location of ~1,340 and ~1,580 cm^{-1} are D peak and G peak, respectively, which attribute to the SP^3 and SP^2 of carbon atoms. The last one at the location of ~2,700 cm^{-1} is the 2D

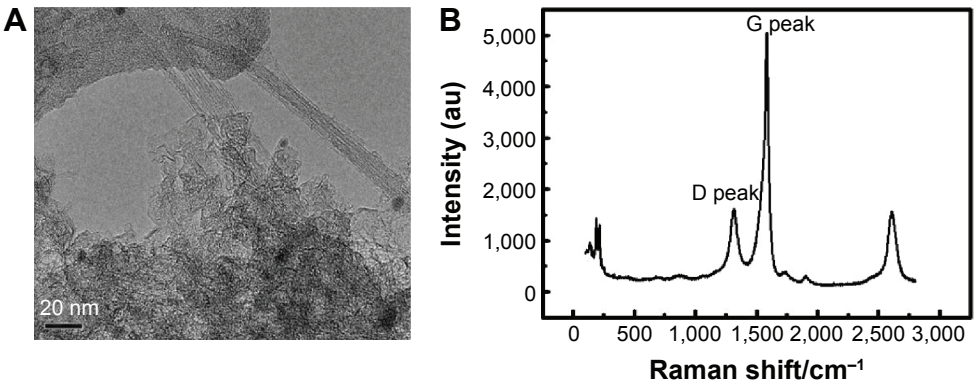

Figure 1 Characterization of G/SWCNT hybrids.
Notes: (**A**) TEM images of G/SWCNT hybrids showing the fibers and particles assembling together. (**B**) Raman spectrum of G/SWCNT hybrids.
Abbreviations: G/SWCNT, graphene/single-walled carbon nanotube; TEM, transmission electron microscopy.

peak of graphene. The results indicate the existence of large amount of graphene and SWCNTs in the hybrids.

Effect of G/SWCNT hybrids on the viability and proliferation of rMSCs

CCK-8 assays measured the number of living cells based on the integrity of mitochondrial function (Figure 2). In Figure 2A, the cytotoxicity of three carbon nanomaterials is observed. At each added concentration of G/SWCNT hybrids, the cells became more viable compared to addition of graphene and SWCNTs. Figure 2B shows the viability and proliferation of cells after treatment with G/SWCNT hybrids at different time points. After treatment for 1 day with G/SWCNT hybrids at a concentration of 20 μg/mL, there was no effect on proliferation. We then examined the effect of the culture period on proliferation. Cells cultured with G/SWCNT hybrids at 10 μg/mL up to 7 days did not show any inhibitory effects on proliferation, but cells treated with G/SWCNT hybrids at a concentration of 20 μg/mL for 7 days inhibited proliferation. The results reveal that treatment of cells with G/SWCNT hybrids at a concentration of 10 μg/mL did not cause inhibitory effects and they still proliferated well. It is important to note that the cell viability was not affected by the presence of G/SWCNT hybrids, since G/SWCNT hybrids are biocompatible.

Effect of G/SWCNT hybrids on the cytoskeleton organization of rMSCs

The structure and morphology of the cells can be used, to some extent, to reflect cellular behavior. Figure 3 displays the fluorescent images of rMSCs treated with G/SWCNT hybrids, which were obtained using immunofluorescence staining. Cells were stained with TRITC-phalloidin to label actin stress fibers (red) and with 4′,6-diamidino-2-phenylindole to label the cell nuclei (blue). Cytochalasin D is a cell-permeable fungal toxin that causes inhibition of actin polymerization.[30] Figure 3B shows that cells pretreated with cytochalasin D for 30 minutes possessed less actin stress fibers compared to the control group (Figure 3A). Following pretreatment with cytochalasin D, no noticeable difference occurred in the red fluorescence signal associated with actin stress fiber formation between the G/SWCNT hybrids (Figure 3D) and the control group after 24 hours of culture. However, cells treated without G/SWCNT hybrids still showed less fluorescence intensity (Figure 3C). The results suggest that G/SWCNT hybrids could enhance actin polymerization.

Effects of G/SWCNT hybrids on the ALP activity of rMSCs

ALP activity assay was used to evaluate the early differentiation status of cells following addition of G/SWCNT hybrids to the osteogenic induction medium. The results of ALP activity were measured by testing normalized to total protein content. NaF was used as the positive control. As shown in Figure 4, the G/SWCNT hybrids promoted the osteogenic differentiation of cells. The results reveal that cells treated with G/SWCNT hybrids showed a significant increase in the ALP content of rMSCs as early as day 7, with more accumulation observed as the cells matured at day 14. G/SWCNT hybrids at different concentrations showed the highest ALP activity after culturing for 14 days than

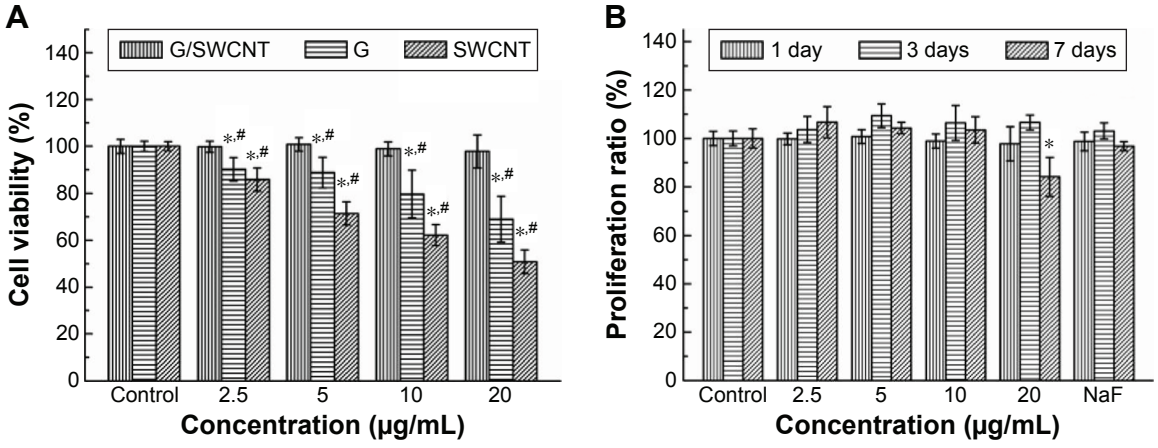

Figure 2 The viability and proliferation of rMSCs after they were treated with different concentrations of carbon nanomaterials.

Notes: (**A**) Cell viability of rMSCs incubated for 24 hours with different concentrations of G/SWCNT hybrids, G, and SWCNTs. (**B**) The proliferation of rMSCs after they were treated with different concentrations of G/SWCNT hybrids for 1, 3, and 7 days. Data represent mean ± SD for n=5. *$P<0.05$ (compared to control) or #$P<0.05$ (compared to the corresponding concentration of the G/SWCNT hybrids).

Abbreviations: G, graphene; G/SWCNT, graphene/single-walled carbon nanotube; NaF, sodium fluoride; rMSCs, rat mesenchymal stem cells; SD, standard deviation; SWCNTs, single-walled carbon nanotubes.

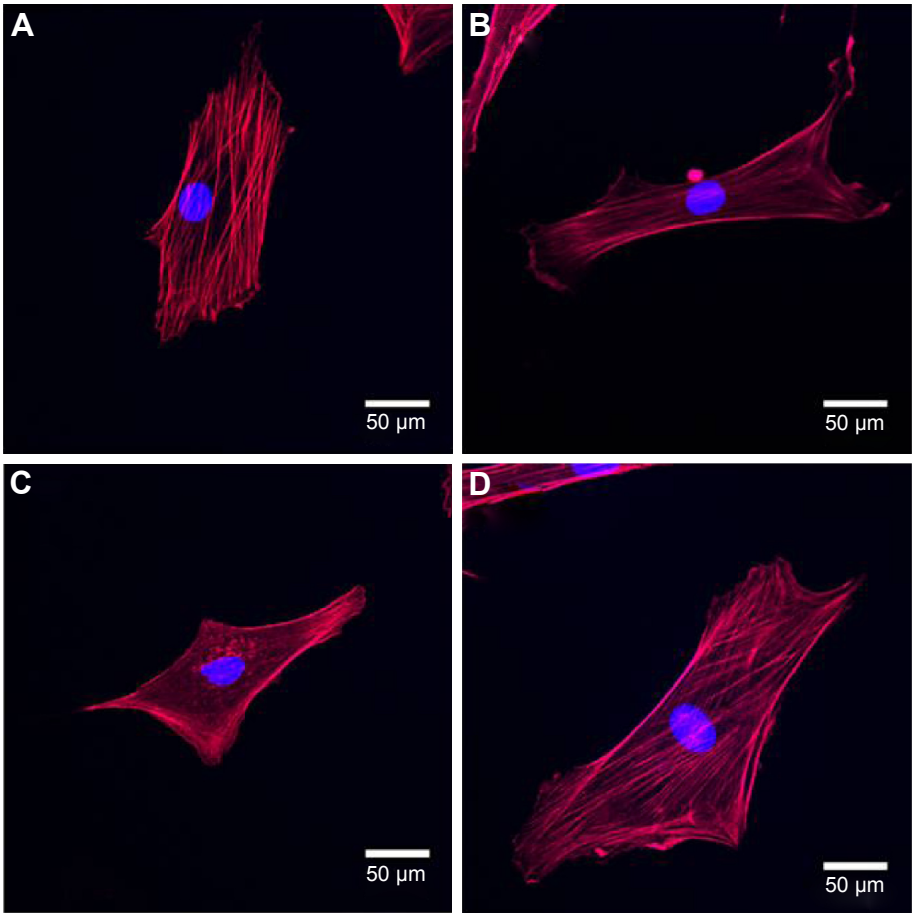

Figure 3 Immunofluorescence images of cytoskeletal organization of rMSCs stained with phalloidin for F-actin (red) and with PI for nuclei (blue).
Notes: (**A**) Cells incubated with culture medium were used as the control group. (**B**) Cells were pretreated with cytochalasin D for 30 minutes and then incubated (**C**) without and (**D**) with G/SWCNT hybrids at a concentration of 10 pg/mL for 24 hours. Scale bar =50 μm.
Abbreviations: G/SWCNT, graphene/single-walled carbon nanotube; PI, propidium iodide; rMSCs, rat mesenchymal stein cells.

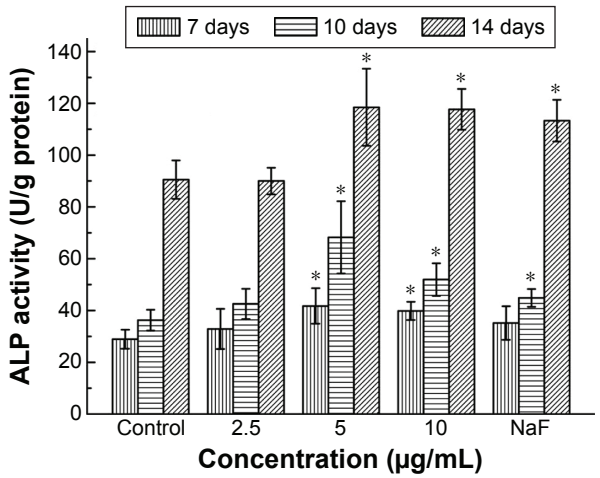

Figure 4 ALP activity of rMSCs treated with different concentrations of G/SWCNT hybrids.
Notes: Cells treated with G/SWCNT hybrids had higher ALP activity, indicating increased cellular differentiation. Data represent mean ± SD for n=4. *$P<0.05$ (compared to control).
Abbreviations: ALP, alkaline phosphatase; G/SWCNT, graphene/single-walled carbon nanotube; NaF, sodium fluoride; rMSCs, rat mesenchymal stem cells; SD, standard deviation.

after culturing for 7 and 10 days. Both G/SWCNT hybrids-treated and NaF-treated groups were able to increase the ALP activity.

Effects of G/SWCNT hybrids on the mineralized matrix nodule of rMSCs

The formation of a mineralized matrix nodule, a marker for the late stage of osteogenic differentiation, was determined by ARS. Figure 5 shows the representative microscopic images of ARS and the semi-quantification results for cells treated with G/SWCNT hybrids. ARS positive staining was found to be much greater after incubating the cells with G/SWCNT hybrids at a concentration of 10 μg/mL for 14 days (Figure 5A–C). There was no mineralized nodule formation in cells that were cultured in regular growth media (Figure 5D), and the quantification results are consistent with the microscopic pictures shown in Figure 5E. G/SWCNT hybrids increased the level of calcium deposition in a

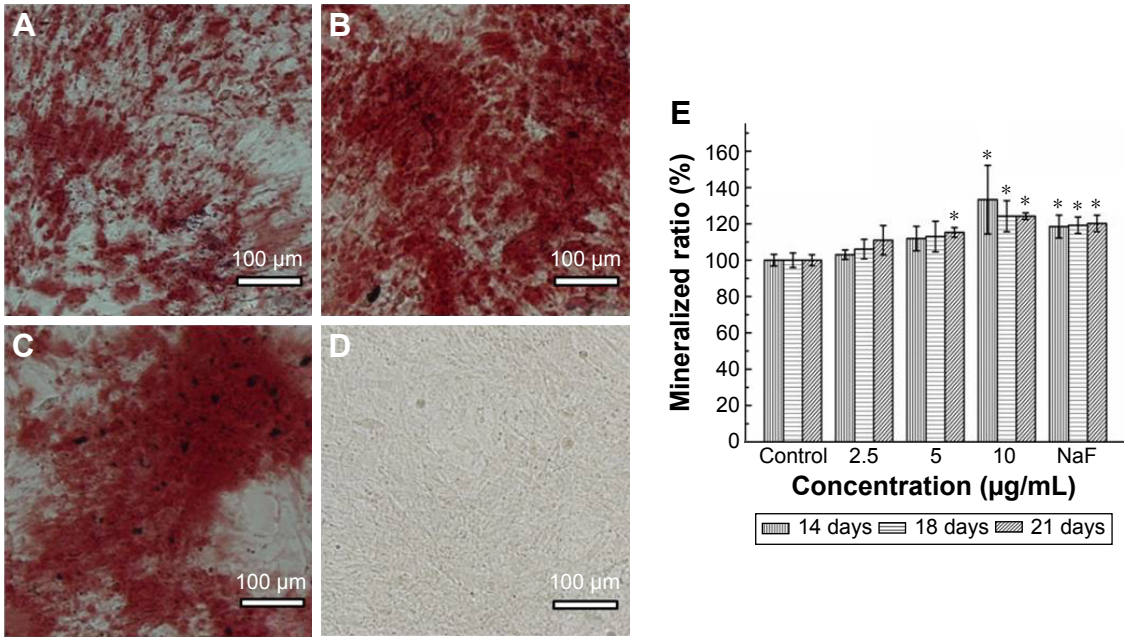

Figure 5 Effect of different concentrations of G/SWCNT hybrids on the mineralized bone nodule of rMSCs.
Notes: Representative images showing ARS of rMSCs treated (**A**) without and (**B**) with G/SWCNT hybrids after 14 days of differentiation. (**C**) NaF treatment was used as a positive control. (**D**) Cells incubated with the culture medium were used as the undifferentiation control. Scale bar =100 μm. (**E**) Mineralization was quantitated by measuring the ARS content of stained calcium deposits. The extracted ARS content confirmed that G/SWCNT hybrids increased extracellular calcium deposition of cells. Data represent the mean ± SD with n=4 for each bar. *$P<0.05$ (compared to control).
Abbreviations: ARS, alizarin red staining; G/SWCNT, graphene/single-walled carbon nanotube; NaF, sodium fluoride; rMSCs, rat mesenchymal stem cells; SD, standard deviation.

dose-dependent manner. G/SWCNT hybrids at a concentration of 10 μg/mL promoted the greatest mineralization; 2.5, 5, and 10 μg/mL of G/SWCNT and NaF promoted mineralization by 103%, 111.9%, 133.3%, and 118.5%, respectively, on day 14. Cells treated with G/SWCNT hybrids deposited an obvious mineralized matrix between day 14 and 21.

Effects of G/SWCNT hybrids on adipogenic differentiation of rMSCs

In Figure 6, it is observed that cells stained with oil red O showed fatty lipid deposits after incubation with G/SWCNT hybrids at concentrations of 2.5, 5, and 10 μg/mL in adipogenic differentiation media. The results reveal that rMSCs cultured with G/SWCNT hybrids and NaF exhibited less staining of adipocytes compared to the control group (Figure 6A–C), but no lipid droplets were observed in the noninduced group (Figure 6D). The quantitative statistical analysis showed a similar trend. Figure 6E displays the semi-quantification of oil red O staining for MSCs cultured at different time points. The data indicate a decrease in adipocyte content after treatment with increasing concentrations of G/SWCNT hybrids; 2.5, 5, and 10 μg/mL of G/SWCNT and NaF inhibited adipogenic differentiation of MSCs by 84%, 77.03%, 71.97%, and 90.27%, respectively, on day 21.

Effects of G/SWCNT hybrids on the expression levels of osteogenic and adipocytic differentiation specific genes

To demonstrate the enhanced osteogenic differentiation of rMSCs with G/SWCNT hybrids, we studied the gene expressions of the differentiated cells, wherein cells that differentiated without G/SWCNT hybrids were used as the control group. Figure 7 shows that all the osteoblast lineage-associated genes, including *OCN*, *OPN*, and *Runx2*, were upregulated in rMSCs in the presence of G/SWCNT hybrids, while the adipose-specific gene *PPARγ2* was downregulated, compared to the control group. In addition, the osteoblast lineage-associated genes showed the highest expression with G/SWCNT hybrids at a concentration of 10 μg/mL, which was greater than in other concentrations and the NaF-treated group. According to these results and as expected, the G/SWCNT hybrids could enhance the differentiation of rMSCs into osteoblasts through upregulation of osteogenic differentiation genes and downregulation of adipogenic differentiation gene.

Western blot analysis of the key proteins involved in MAPK signaling pathway

The mechanism of the differentiation processes, which possibly account for the observed effects of MAPK signaling

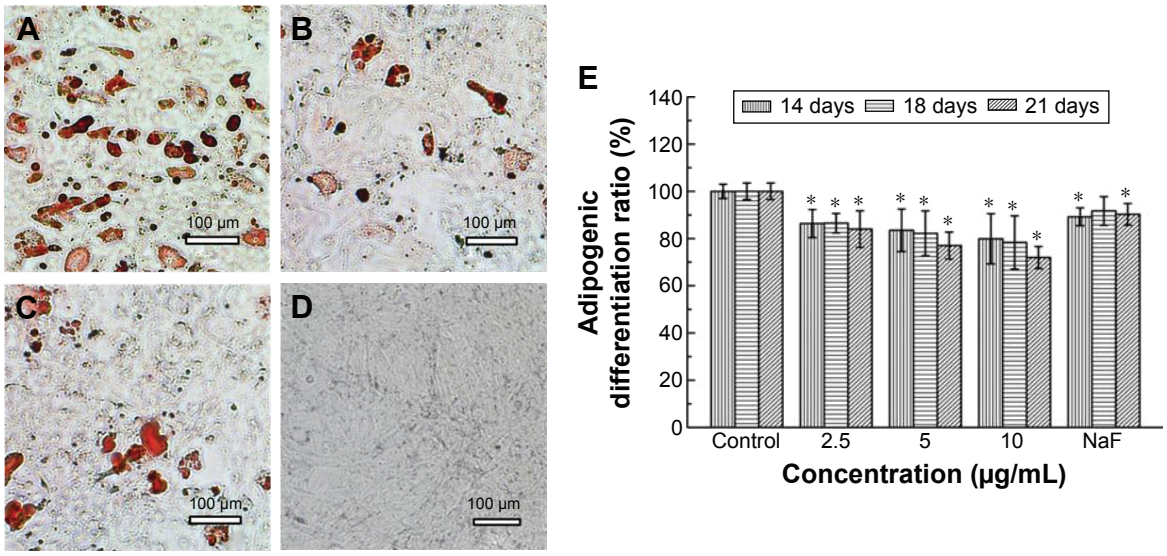

Figure 6 Evaluation of adipogenic differentiation of rMSCs after they were treated with G/SWCNT hybrids.
Notes: Representative images showing oil red O staining of adipocytes treated (**A**) without and (**B**) with G/SWCNT hybrids after 21 days of differentiation. (**C**) NaF treatment was used as a positive control. (**D**) Cells incubated with culture medium were used as the undifferentiation control. Scale bar =100 μm. (**E**) Adipocytes were quantitated by measuring oil red O from the stained cytoplasmic lipid accumulation. The results demonstrated G/SWCNT hybrids inhibited adipogenic differentiation of rMSCs. Data represent the mean ± SD with n=4 for each bar. *$P<0.05$ (compared to control).
Abbreviations: G/SWCNT, graphene/single-walled carbon nanotube; NaF, sodium fluoride; rMSCs, rat mesenchymal stem cells; SD, standard deviation.

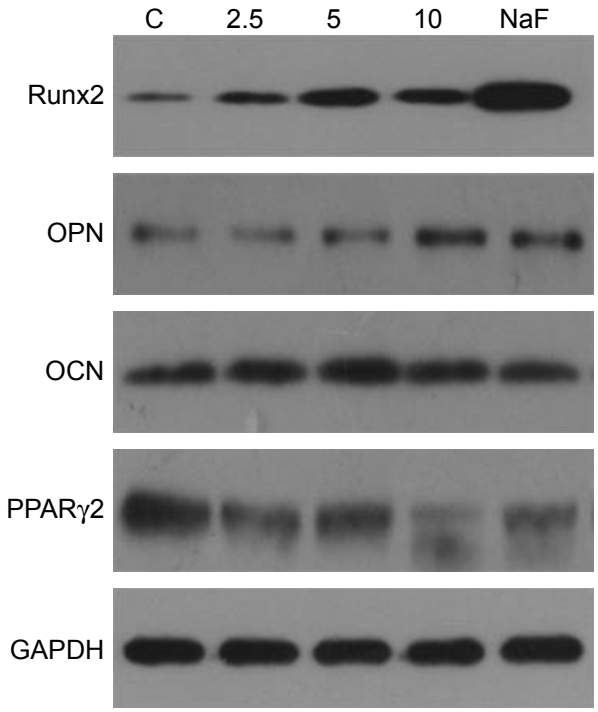

Figure 7 Western blot analysis for the expression levels of osteogenic and adipogenic differentiation specific genes in rMSCs treated with G/SWCNT hybrids after differentiation.
Notes: NaF-treated group served as positive control. After treatment with G/SWCNT hybrids, the expression levels of osteogenic genes, including *Runx2*, *OCN*, and *OPN*, were upregulated, while the adipose-specific gene, *PPARγ2*, was downregulated.
Abbreviations: C, control; GAPDH, glyceraldehyde-3-phosphate dehydrogenase; G/SWCNT, graphene/single-walled carbon nanotube; NaF, sodium fluoride; OCN, osteocalcin; OPN, osteopontin; PPARγ2, peroxisome proliferator-activated receptor-γ2; rMSCs, rat mesenchymal stem cells; Runx2, runt-related transcription factor 2.

pathways, is shown in Figure 8. It is notable that the genes related to the MAPK cellular signaling pathways, such as p38, were significantly upregulated and ERK1/2 was downregulated when rMSCs were treated with G/SWCNT hybrids.

Discussion

Following osteogenic induction, MSCs could be used to mimic the course of osteogenic differentiation in vitro based on their biological properties, including easy isolation and expansion, and could minimize substantial risks for host rejection.[31] The ability to control the differentiation of MSCs into osteoblasts is crucial for effective bone engineering and regeneration. Carbon nanomaterials, in particular, have emerged as a promising platform with potential use in biological applications, mainly because of their intriguing physiochemical properties and the natural existence of carbon in the human body.[32] It is noteworthy that carbon nanomaterials could modulate the differentiation of cells toward osteogenic differentiation. In this study, we found that G/SWCNT hybrids could enhance such beneficial osteogenic differentiation of rMSCs.

The cytotoxicity of G/SWCNT hybrids was initially measured by cell proliferation assay and morphology observations. Previous studies have suggested that carbon nanomaterials present high level of biocompatibility toward MSCs and osteoblasts.[19,33] Our results show that the cytotoxicity of G/SWCNT hybrids was less than that of graphene and

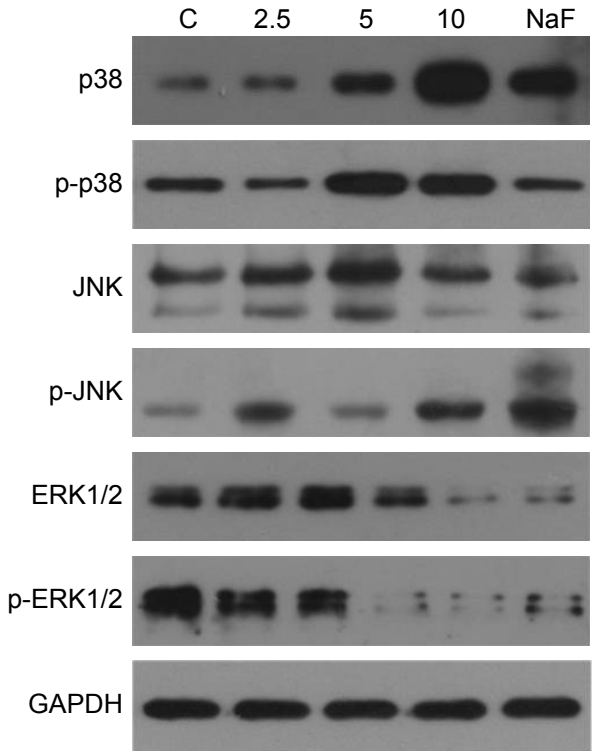

Figure 8 Western blot analysis for the expression levels of MAPK signaling pathway genes in rMSCs treated with G/SWCNT hybrids after differentiation.
Notes: The expression level of p38 was upregulated and ERK1/2 was downregulated in rMSCs in the presence of G/SWCNT hybrids.
Abbreviations: C, control; ERK1/2, extracellular signal-regulated protein kinases; GAPDH, glyceraldehyde-3-phosphate dehydrogenase; G/SWCNT, graphene/single-walled carbon nanotube; MAPK, mitogen-activated protein kinase; p-, phospho-; p38, p38 MAP kinase; rMSCs, rat mesenchymal stein cells.

SWCNTs, and there were no significant differences in cell viability and no deleterious effects on the cells after treatment with G/SWCNT hybrids in concentrations up to 10 μg/mL. The data also demonstrate that treatment with G/SWCNT hybrids provides a suitable environment for the rMSCs to remain viable. It can be also assumed that proliferation of cells was not affected by the nanomaterial. Following cell proliferation, osteogenic differentiation occurs as a sequential event. On the other hand, the concentration of G/SWCNT hybrids in the following experiments could be confrmed. Cells treated with G/SWCNT hybrids proliferated, but no significant increase was observed with an increase in incubation time, compared to the control group. These results demonstrate that enhanced osteogenic differentiation did not occur because of the increased rate of cell proliferation, and rMSCs could be potentially treated with G/SWCNT hybrids at a concentration of 10 μg/mL.

It has been reported that the morphological alteration of cells is related to their ability of being multipotential.[34,35] Cells were stained simultaneously with TRITC-conjugated phalloidin to reveal actin filaments and with propidium iodide in order to detect the cell nucleus. After pretreatment with cytochalasin D, cells incubated with G/SWCNT hybrids proved to be richer in actin filaments than those incubated without G/SWCNT hybrids. The immunofluorescent staining results suggest that treatment with G/SWCNT hybrids may result in faster rate of repair compared to the untreated group.

Although the viability of cells is an indicator of initial biocompatibility, it may not predict the differentiation of MSCs that follows. To determine the effect of G/SWCNT hybrids on the osteogenic differentiation, rMSCs were characterized by measuring differentiation markers, including ALP, and the formation of mineralized matrix nodules. ALP, a predictor of osteoblast formation, is a highly specific marker of osteoblasts function and bone formation. Our results demonstrate that G/SWCNT hybrids lead to an increased expression of osteogenic differentiation markers at different time points compared to the control group, especially at day 14. Previous studies have demonstrated that ALP activity increased as the culture coursed toward early mineralization phase of cells where they differentiated into preosteoblasts and osteoblasts.[29] Both G/SWCNT hybrid-treated and NaF-treated groups were able to increase the ALP activity. Similar effects of other carbon nanomaterials have been reported in previous studies. Oxygen plasma-treated SWCNT substrates enhanced the expression of ALP of human MSCs in the early days of culture.[35] ALP of the SaoS2 cells cultured on multi-walled carbon nanotube compacts was at a significantly higher level at each culture time point.[36]

The formation of mineralized matrix nodules is an essential sign of osteogenic differentiation of MSCs. ARS assay was used to measure the mineralized matrix nodules, and semi-quantification of the amount was achieved by dissolution from stained calcium deposit. Similar to that of ALP activity assay, ARS staining revealed an obvious osteogenic differentiation potential after induction in the presence of G/SWCNT hybrids at all time points. The staining results also showed that the cells were fully mature as there was a high intensity of staining, which indicated the presence of calcium deposits due to the mineralized nodule formation. The semi-quantitative results further confirmed that cells treated with G/SWCNT hybrids exhibited a higher degree of mineralization potential toward the osteogenic lineage, compared to the control group. Notably, more of the rMSCs treated with G/SWCNT hybrids developed into osteoblasts by promoting early stage osteogenic differentiation and late stage mineralized matrix nodule formation, compared to the control group. This may be attributed to graphene, which has the ability to preconcentrate the growth factors

and osteogenic inducers, including β-glycerolphosphate, dexamethasone, and ascorbic acid.[20,37] Previous literature reports demonstrated that increasing concentrations of dexamethasone along with β-glycerolphosphate can enhance osteogenic differentiation through interaction with intracellular ALP enzymes.[38] Dexamethasone could be absorbed by a graphite structure by π–π bonding, and ascorbic acid also aids in the formation of mature osteoblasts that could interact with carbon nanomaterials through hydrogen bonding.[39]

Notably, the biological response between cells and materials is not only affected by their chemistry, but also by their structure.[36,40] The structure of nanomaterials is a major contributing factor that determines their surface properties, since cells can interact with nanomaterial surfaces immediately. Although both graphene and SWCNTs are isomorphs of pure carbon, it has been indicated that graphene and SWCNTs are expected to exhibit high surface area in G/SWCNT hybrids. In other words, G/SWCNT hybrids with larger surface areas could adsorb more osteogenic inducers and proteins from the culture medium, so G/SWCNT hybrids considered to be "osteogenic inducers sorbent" might enhance the differentiation of cells. On the other hand, the adsorption of osteogenic inducers and proteins might alter the surface energy, and the enhanced surface energy could promote the initial cell attachment and the following proliferation.[7]

MSCs are pluripotent and can differentiate into distinct cell lineages, including osteoblasts and adipocytes. Increasing evidence has demonstrated that MSCs enter the osteogenic pathway when the adipogenic pathway is blocked and vice versa.[41] Because of the reciprocal relationship between osteogenic and adipogenic differentiation of MSCs, we examined whether the promotion of osteoblast differentiation occurred due to the inhibition of adipogenic differentiation. The oil red O staining assay showed that cells treated with G/SWCNT hybrids had less staining of fatty lipid deposits, which was confirmed both visually and by quantification analysis. The adipogenic differentiation was inhibited when rMSCs were treated with adipogenic induction media in the presence of G/SWCNT hybrids.

Overall, the G/SWCNT hybrids have proven to greatly enhance osteogenic differentiation of rMSCs. To further confirm our findings and to demonstrate the underlying mechanism of G/SWCNT hybrid-mediated cell behavior, we analyzed the expression levels of osteogenic and adipogenic differentiation specific genes and intracellular pathway studies. *Runx2* is a master regulator gene of osteogenic differentiation.[42] OCN and OPN are regarded as the specific markers of mineralization and matrix maturation of the osteoblasts, which accumulate in mineralized bone and occur due to increased phosphate and calcium levels that induce spontaneous mineralization.[43,44] Results indicate that the expression levels of the osteogenic commitment gene *Runx-2*, as well as other osteogenic phenotype genes including *OCN* and *OPN*, were all increased in cells treated with G/SWCNT hybrids as compared to the control group. This further indicates the enhancement of osteogenic differentiation of rMSCs after treatment with G/SWCNT hybrids. These results are consistent with those of ALP activity and ARS staining, which are other markers for the formation of osteoblasts.

The expression level of PPARγ2 was down-regulated, which plays an important role in modulating the adipogenic differentiation of MSCs.[22] Based on the gene expression data, it was further confirmed that G/SWCNT hybrids could promote osteogenic differentiation and not adipogenic lineage of rMSCs, as evidenced by the upregulation of the osteogenic lineage-associated markers and downregulation of the adipogenic differentiation marker.

Compared to the control group, enhanced synthesis of ALP, deposition of mineralized matrix nodule, as well as decreased formation of fatty lipid deposits were observed in rMSCs treated with G/SWCNT hybrids. In this manner, our results demonstrate that combination of the nanostructure materials in G/SWCNT hybrids, together with the effective differentiation of stem cells into osteoblasts, could lay the foundation for potential applications in bone regenerative medicine. However, stem cell differentiation is activated or inhibited by specific signaling pathways. In order to better understand bone development and disease, elucidating the signaling pathways by which osteogenic differentiation is driven by G/SWCNT hybrids is necessary.

We seek to further understand the signaling pathways by which G/SWCNT hybrids control cell fate and modulate the differentiation of MSCs into the osteogenic lineage. The MAPK mediates the response of cells to many extracellular stimuli, including two stress-activated protein kinases, p38 MAPK (p38) and JNK, and ERK. The three related MAPK pathways contribute to multiple cellular processes, such as proliferation, survival, and differentiation, that mediate the response of cells to extracellular stimuli.[45] p38 has shown to act as a coactivator to regulate *Runx2* gene expression during mesenchymal precursor cell differentiation.[46,47] Combining all results, our data demonstrate that the p38 signaling pathway plays a positive role in enhancing osteogenic differentiation of MSCs with respect to G/SWCNT hybrid interactions. We hypothesize that the enhanced differentiation of cells by G/SWCNT hybrids is modulated through the MAPK

signaling pathway. Activation of the p38 signaling pathway and inhibition of the ERK1/2 signaling pathway lead to upregulation of osteoblast-related genes and downregulation of adipocytic differentiation genes, which further enhance the osteogenic differentiation of rMSCs.

Conclusion

In this study, the MSCs were derived from rat bone marrow and cultured with G/SWCNT hybrids for the first time. We found that the presence of G/SWCNT hybrids significantly affects the cell behavior and subsequent expression levels of genes involved in osteogenic and adipogenic differentiation. Our results suggest that G/SWCNT hybrids do not affect the viability of MSCs. Furthermore, G/SWCNT hybrids enhanced the osteogenic differentiation of rMSCs, while also inhibiting the differentiation toward adipocytes. This will lay the foundation for applying G/SWCNT hybrids as potential nanodelivery carriers and tissue engineering scaffolds that could influence the differentiation of rMSCs for enhancing bone formation. Overall, we envision that the combination of G/SWCNT hybrids and the effective differentiation of stem cells toward osteoblasts could pave the way toward a wide range of applications implementing this carbon nanomaterial for bone regeneration and tissue engineering.

Acknowledgments

This work was supported by the National Natural Science Foundation of China (81302344, 81401573, and 81371973), the Chenguang Project from Wuhan Science and Technology Bureau (2014070404010221), and the Wuhan Municipal Health and Family Planning Commission Foundation of China (WX15C10).

Disclosure

The authors report no conflicts of interest in this work.

References

1. Pittenger MF, Mackay AM, Beck SC, et al. Multilineage potential of adult human mesenchymal stem cells. *Science*. 1999;284(5411):143–147.
2. Uccelli A, Moretta L, Pistoia V. Mesenchymal stem cells in health and disease. *Nat Rev Immunol*. 2008;8(9):726–736.
3. Hsiao YS, Kuo CW, Chen P. Multifunctional graphene-PEDOT microelectrodes for on-chip manipulation of human mesenchymal stem cells. *Adv Funct Mater*. 2013;23(37):4649–4656.
4. Ciofani G, Ricotti L, Canale C, et al. Effects of barium titanate nanoparticles on proliferation and differentiation of rat mesenchymal stem cells. *Colloid Surf B*. 2013;102:312–320.
5. Cao W, Cao K, Cao J, Wang Y, Shi Y. Mesenchymal stem cells and adaptive immune responses. *Immunol Lett*. 2015;168(2):147–153.
6. Ciapetti G, Ambrosio L, Marletta G, Baldini N, Giunti A. Human bone marrow stromal cells: in vitro expansion and differentiation for bone engineering. *Biomaterials*. 2006;27(36):6150–6160.
7. Li X, Liu H, Niu X, et al. The use of carbon nanotubes to induce osteogenic differentiation of human adipose-derived MSCs in vitro and ectopic bone formation in vivo. *Biomaterials*. 2012;33(19):4818–4827.
8. Yi C, Liu D, Fong C, Zhang J, Yang M. Gold nanoparticles promote osteogenic differentiation of mesenchymal stem cells through p38 MAPK pathway. *ACS Nano*. 2010;4(11):6439–6448.
9. Liu Y, Dong X, Chen P. Biological and chemical sensors based on graphene materials. *Chem Soc Rev*. 2012;41(6):2283–2307.
10. Barone PW, Baik S, Heller DA, Strano MS. Near-infrared optical sensors based on single-walled carbon nanotubes. *Nat Mater*. 2005;4(1):86–92.
11. Shen H, Zhang L, Liu M, Zhang Z. Biomedical applications of graphene. *Theranostics*. 2012;2(3):283–294.
12. Heister E, Neves V, Tîlmaciu C, et al. Triple functionalisation of single-walled carbon nanotubes with doxorubicin, a monoclonal antibody, and a fluorescent marker for targeted cancer therapy. *Carbon*. 2009;47(9):2152–2160.
13. Liu Z, Robinson JT, Tabakman SM, Yang K, Dai H. Carbon materials for drug delivery & cancer therapy. *Mater Today*. 2011;14(7):316–323.
14. Ji SR, Liu C, Zhang B, et al. Carbon nanotubes in cancer diagnosis and therapy. *Biochim Biophys Acta*. 2010;1806(1):29–35.
15. Lee JH, Shim W, Choolakadavil KN, et al. Random networks of single-walled carbon nanotubes promote mesenchymal stem cell's proliferation and differentiation. *ACS Appl Mater Inter*. 2015;7(3):1560–1567.
16. Goenka S, Sant V, Sant S. Graphene-based nanomaterials for drug delivery and tissue engineering. *J Control Release*. 2014;173(1):75–88.
17. Zhao MQ, Zhang Q, Huang JQ, et al. Towards high purity graphene/single-walled carbon nanotube hybrids with improved electrochemical capacitive performance. *Carbon*. 2013;54(2):403–411.
18. Zhao MQ, Liu XF, Zhang Q, et al. Graphene/single-walled carbon nanotube hybrids: one-step catalytic growth and applications for high-rate Li-S batteries. *ACS Nano*. 2012;6(12):10759–10769.
19. Nayak TR, Andersen H, Makam VS, et al. Graphene for controlled and accelerated osteogenic differentiation of human mesenchymal stem cells. *ACS Nano*. 2011;5(6):4670–4678.
20. Akhavan O, Ghaderi E, Shahsavar M. Graphene nanogrids for selective and fast osteogenic differentiation of human mesenchymal stem cells. *Carbon*. 2013;59(7):200–211.
21. Khang D, Choi J, Im YM, et al. Role of subnano-, nano- and submicron-surface features on osteoblast differentiation of bone marrow mesenchymal stem cells. *Biomaterials*. 2012;33(26):5997–6007.
22. Liu D, Yi C, Wang K, et al. Reorganization of cytoskeleton and transient activation of Ca^{2+} channels in mesenchymal stem cells cultured on silicon nanowire arrays. *ACS App Mater Inter*. 2013;5(24):13295–13304.
23. Huang Y, Zhou G, Zheng L, Liu H, Niu X, Fan Y. Micro-/nano-sized hydroxyapatite directs differentiation of rat bone marrow derived mesenchymal stem cells towards an osteoblast lineage. *Nanoscale*. 2012;4(7):2484–2490.
24. Kim KJ, Joe YA, Kim MK, et al. Silica nanoparticles increase human adipose tissue-derived stem cell proliferation through ERK1/2 activation. *Int J Nanomed*. 2015;10:2261–2272.
25. Zarubin T, Han J. Activation and signaling of the p38 MAP kinase pathway. *Cell Res*. 2005;15(1):11–18.
26. Guicheux J, Lemonnier J, Ghayor C, Suzuki A, Palmer G, Caverzasio J. Activation of p38 mitogen-activated protein kinase and c-Jun-NH2-terminal kinase by BMP-2 and their implication in the stimulation of osteoblastic cell differentiation. *J Bone Miner Res*. 2003;18(11):2060–2068.
27. Suzuki A, Guicheux J, Palmer G, et al. Evidence for a role of p38 MAPK kinase in expression of alkaline phosphatase during osteoblastic cell differentiation. *Bone*. 2002;30(1):91–98.
28. Maniatopoulos C, Sodek J, Melcher AH. Bone formation in vitro by stromal cells obtained from bone marrow of young adult rats. *Cell Tissue Res*. 1988;254(2):317–330.
29. Farley JR, Wergedal JE, Baylink DJ. Fluoride directly stimulates proliferation and alkaline phosphatase activity of bone-forming cells. *Science*. 1983;222(4621):330–332.

30. Wakatsuki T, Schwab B, Thompson NC, Elson EL. Effects of cytochalasin D and latrunculin B on mechanical properties of cells. *J Cell Sci*. 2001;114(Pt 5):1025–1036.
31. Strauer BE, Kornowski R. Stem cell therapy in perspective. *Circulation*. 2003;107(7):929–934.
32. Brammer KS, Choi C, Frandsen CJ, Oh S, Johnston G, Jin S. Comparative cell behavior on carbon-coated TiO_2 nanotube surfaces for osteoblasts vs. osteo-progenitor cells. *Acta Biomater*. 2011;7(6):2697–2703.
33. Rodrigues BV, Leite NC, Cavalcanti Bd, et al. Graphene oxide/multi-walled carbon nanotubes as nanofeatured scaffolds for the assisted deposition of nanohydroxyapatite: characterization and biological evaluation. *Int J Nanomed*. 2016;11:2569–2585.
34. Rodriguez JP, Gonzalez M, Rios S, Cambiazo V. Cytoskeletal organization of human mesenchymal stem cells (MSC) changes during their osteogenic differentiation. *J Cell Biochem*. 2004;93(4):721–731.
35. Baik KY, Park SY, Heo K, Lee KB, Hong S. Carbon nanotube monolayer cues for osteogenesis of mesenchymal stem cells. *Small*. 2011;7(6):741–745.
36. Li X, Gao H, Uo M, et al. Maturation of osteoblast-like SaoS2 induced by carbon nanotubes. *Biomed Mater*. 2009;4(1):015005.
37. Lee WC, Lim CH, Shi H, et al. Origin of enhanced stem cell growth and differentiation on graphene and graphene oxide. *ACS Nano*. 2011;5(9):7334–7341.
38. Jaiswal N, Haynesworth SE, Caplan AI, Bruder SP. Osteogenic differentiation of purified, culture-expanded human mesenchymal stem cells in vitro. *J Cell Biochem*. 1997;64(2):295–312.
39. Quarles LD, Yohay DA, Lever LW, Caton R, Wenstrup RJ. Distinct proliferative and differentiated stages of murine MC3T3-E1 cells in culture: an in vitro model of osteoblasts development. *J Bone Miner Res*. 1992;7(6):683–692.
40. Li X, Van Blitterswijk CA, Feng Q, Cui F, Watari F. The effect of calcium phosphate microstructure on bone-related cells in vitro. *Biomaterials*. 2008;29(23):3306–3316.
41. Zhang W, Yang N, Shi XM. Regulation of mesenchymal stem cell osteogenic differentiation by glucocorticoid-induced leucine zipper (GILZ). *J Biol Chem*. 2008;283(8):4723–4729.
42. Liu D, Zhang J, Wang G, Liu X, Wang S, Yang M. The dual-effects of LaCl(3) on the proliferation, osteogenic differentiation, and mineralization of MC3T3-E1 cells. *Biol Trace Elem Res*. 2012;150(1–3):433–440.
43. Owen TA, Aronow M, Shalhoub V, et al. Progressive development of the rat osteoblast phenotype in vitro: reciprocal relationships in expression of genes associated with osteoblast proliferation and differentiation during formation of the bone extracellular matrix. *J Cell Physiol*. 1990;143(3):420–430.
44. Kasugai S, Nagata T, Sodek J. Temporal studies on the tissue compartmentalization of bone sialoprotein (BSP), osteopontin (OPN), and SPARC protein during bone formation in vitro. *J Cell Physiol*. 1992;152(3):457–477.
45. Chang L, Karin M. Mammalian MAP kinase signalling cascades. *Nature*. 2001;410(6824):37–40.
46. Chaudhary LR, Avioli LV. Extracellular-signal regulated kinase signaling pathway mediates downregulation of type I procollagen gene expression by FGF-2, PDGF-BB, and okadaic acid in osteoblastic cells. *J Cell Biochem*. 2000;76(3):354–359.
47. Lee KS, Hong SH, Bae SC. Both the Smad and p38 MAPK pathways play a crucial role in Runx2 expression following induction by transforming growth factor-beta and bone morphogenetic protein. *Oncogene*. 2002;21(47):7156–7163.